RELATIONSHIP BETWEEN THERMAL CONDUCTIVITY AND TENSILE STRENGTH IN CAST IRONS

Vasilios Fourlakidis, Juan Carlos Hernando and Attila Diószegi
School of Engineering, Department of Materials and Manufacturing, Jönköping University, Jönköping, Sweden

Daniel Holmgren
Tenneco Inc. Greater Gothenburg Metropolitan Area, Gothenburg, Sweden

https://doi.org/10.1007/s40962-023-00970-6

Abstract

Improved mechanical and thermal properties are important characteristics for enhancing the performance of cast iron components that operate at elevated temperatures. Thermal conductivity defines the temperature distribution within the casting and influences the magnitude of the thermally induced tensile stresses. The microstructural features that increase the thermal conductivity have a negative impact on tensile strength. The results reported in this work show that there is a unique inverse relationship between thermal conductivity and tensile strength, valid for the whole range of cast iron alloys regardless of graphite form, solidification rates, carbon content and matrix constituents. The finding indicates the challenges for the simultaneous improvement of these properties, and it can be utilized as a guideline during the design of cast iron components for high temperature applications.

Keywords: *cast iron, thermal conductivity, ultimate tensile strength, component casting*

Introduction

Cast irons are the chosen alloys for manufacturing cylinder heads and cylinder blocks in heavy-duty engines. The technical strategy to enhance engine efficiency involves the increase of the combustion pressure accompanied by the rise of the operational temperature that induces additional thermal stresses.[1] The magnitude of the thermal stresses depends on the peak temperature and the temperature gradient throughout the component and consequently is influenced by the thermal conductivity.[2] The periodically generated thermal stresses induce deformations and tensile stresses on the component and result in thermal fatigue failure. Thus, thermal conductivity and tensile strength influence the thermal fatigue resistance considerably[3] although other phenomena such as the surface degradation due to oxidation also contribute to the reduced life span of the cast iron engine components that operate at high temperatures.[4,5]

Graphite morphology, microstructure constituents and micro-segregation of the alloying elements are the factors that determine cast iron thermal conductivity. Lamellar graphite iron (LGI) has higher thermal conductivity than compacted and spherical graphite iron (CGI and SGI). This difference is due to the predominant growth direction of the graphite particles. Pure ferrite has relatively high thermal conductivity ($\sim$80 Wm^{-1} K^{-1}), and its value decreases with the addition of alloying elements. The pearlite exhibits relatively low conductivity (23–45 $Wm^{-1}K^{-1}$).[6] The cast irons ultimate tensile strength or, in shorten, tensile strength can range between 220 and more than 1000 MPa, depending on the microstructure coarseness, graphite form, matrix structure, alloying elements and other metallurgical and heat treatment conditions.[7] The thermal conductivity and tensile strength of cast iron alloys have been investigated and reported previously by the authors.[8–11] The present work focuses on reporting the direct relation between the thermal and tensile property for a wide range of process parameters that influence these properties such as carbon content, solidification time, graphite morphology and ferrite–pearlite content.

Received: 05 December 2022 / Accepted: 13 January 2023 /
Published online: 2 February 2023

Experimental Procedure

Two different experimental procedures, a sand-casting experiment and a re-melting experiment, were employed for the production of the investigated material.

Description of the casting experiments have been reported in the past.[8,9] Briefly, three different materials (steel, insulation material and sand) surround the experimental castings aimed to provide three different microstructure coarseness. The solidification time of the melt in the chill, sand and insulation material was roughly 80, 400 and 1500 s, respectively. The layout of the sand-casting experiment is depicted in Figure 1.

Cast iron alloys with varying carbon equivalent (CE) and Mg-treatments were produced in the casting experiments. As can be seen in Table 1, different cast iron alloys were treated with four different Mg levels aimed to generate different graphite morphologies in C1 experiment. A fully pearlitic LGI alloy with CE that ranges from hypoeutectic to nearly eutectic composition utilized in C2 experiment.

A re-melting experiment was performed for the production of CGI and SGI samples with controlled nodularity. Table 1 shows the chemical composition of the base alloy used in the C3 experiment. In this experiment, the SGI base alloy was re-melted and held under isothermal conditions to produce samples with nodularity ranging from 0 to 85%. The cooling rate during the solidification is similar for all the samples, and the only variable controlled is the Mg-level. This is done by modifying the holding time at 1450 °C during the re-melting cycle. A detailed description of the experimental technique is presented in.[13]

Thermal conductivity (k) at room temperature was calculated by the thermal diffusivity (α), density (ρ), and specific heat (C_p):

$$k = \alpha \cdot \rho \cdot C_p \qquad \text{Eqn. 1}$$

A Netzsch LFA 427 laser flash apparatus was applied to investigate thermal diffusivity (α). The front surface of the cylindrical sample was heated by a light pulse, and an sensor registered the temperature increase on the back side of the specimen. The thermal diffusivity is given by Eqn. 3:

$$\alpha = C \cdot \frac{l^2}{t_{0.5}} \qquad \text{Eqn. 2}$$

where l is the sample thickness, C is a dimensionless constant, and $t_{0.5}$ is the time needed for a 50% temperature increase at the rear surface of the specimen. Coin shape samples were employed in diffusivity measurements. The dimensions of the samples were Ø10×5 mm. The thermal diffusivity measurements accuracy is ±3%.

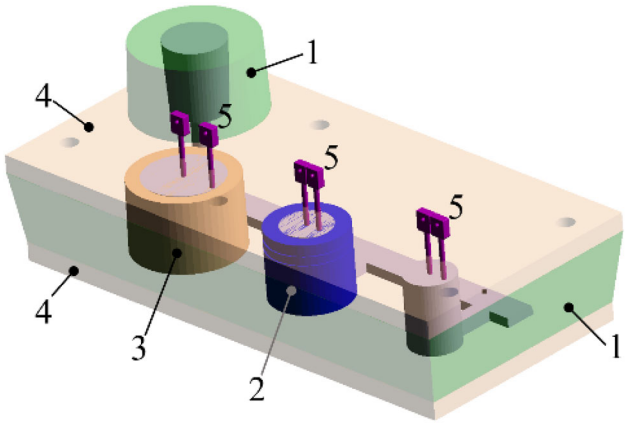

Figure. 1. The experimental layout: (1) sand mold, (2) steel cylinder (chill), (3) cylindrical insulation material, (4) insulation plates, (5) thermocouples. Figure adapted from.[12]

The C_p was measured in a Netzsch DSC 404C Pegasus differential scanning calorimeter. The samples were heated under a protective gas atmosphere with a heating rate of 10 °C/min, and the heat flow into the sample was compared with the heat flow into a sapphire reference sample with known C_p for the estimation of the specific heat. The apparatus has an estimated accuracy of ±2.5%, and the assessed specimens had a weight of 83–84 mg.

The tensile strength from the sand-casting experiment was measured in a MTS tensile test system, according to SS-EN 10 002-1 standard. The tensile specimens' dimensions were 35mm in gauge length and 7 mm in diameter. The tensile strength of CGI and SGI samples from the re-melting experiment has been determined in a Kammrath and Weiss testing module. In this later case, flat miniaturized tensile test bars were used with dimensions of 12 mm gauge length and 2 mm thickness.

Results and Discussion

The samples from experiment C1 (Heat 1-3) and C2 (all Heats) are LGI alloys with type A graphite at low and medium cooling rates. The fast-cooling rate produced fine inter-dendritic graphite. All the samples are of a pearlitic matrix. The samples from experiment C1, Heat 4 and 5, contain compacted and spheroidal graphite with different values of nodularity. The nodularity increased at higher Mg levels in combination with lower S contents. Also, an increasing nodularity was observed for increasing cooling rates. Micrographs of the graphite morphology have been presented in.[8,9]

The chosen cooling conditions in sand-casting experiments (C1 and C2) provided a sizeable variation of microstructure coarseness. Typical primary austenite microstructure from C2-Heat 1 alloy is presented in Figure 2. The etching

Table 1. Chemical Composition (wt%) for the Casting and Re-Melting Experiments (CE=%C+%Si/3+%P/3)

Experiment	Heat	C	Si	Mn	P	S	Cr	Cu	Mg	CE
C1-casting	1	3.32	1.93	0.57	0.04	0.08	0.09	0.18	0.002	4.00
	2	3.21	2.27	0.55	0.03	0.06	0.09	0.18	0.017	4.00
	3	3.19	3.05	0.56	0.03	0.05	0.09	0.18	0.067	4.20
	4	3.05	3.41	0.56	0.04	0.04	0.09	0.18	0.070	4.20
	5	2.99	3.59	0.56	0.04	0.04	0.09	0.18	0.071	4.20
C2-casting	1	3.62	1.88	0.57	0.04	0.08	0.14	0.38	–	4.26
	2	3.34	1.83	0.56	0.04	0.08	0.15	0.37	–	3.96
	3	3.05	1.77	0.54	0.04	0.08	0.14	0.36	–	3.65
	4	2.80	1.75	0.54	0.04	0.08	0.15	0.35	–	3.40
C3-re-melting		3.33	2.64	0.69	0.03	0.01	0.08	0.86	0.063	4.22

reagent contains picric acid, NaOH, KOH and distilled water (1:1:4:5 ratio, respectively), and the etching is performed at 110 °C.

Typical microstructures from the samples produced after the re-melting experiments, C3, are shown in Figure 3. As we can observe in Figure 3(a), for 10 min holding time, the nodularity is over 80% and the matrix is fully pearlitic. After 60 min holding time, the nodularity drops to 10% (CGI), see Figure 3(b). After 150 min holding time, the graphite microstructure becomes lamellar (LGI), as shown in Figure 3(c). The ferrite content increases with the holding time.

Figure 4 illustrates the relation between tensile strength and thermal conductivity as a function of nodularity at room temperature. The thermal conductivity decreases, and tensile strength increases with an increasing nodularity. This relation shows how the increase in one property implies the decrease of the other.

The wide range of CE, Mg-content and cooling rates that were utilized in this work produced a wide variation of graphite forms, microstructure constituents and structure coarseness. This wide experimental ensemble results in tensile strength and thermal conductivities that range between 180 and 650 MPa and 20–65 $Wm^{-1}K^{-1}$, respectively, and covers largely the property spectrum of LGI, CGI and SGI. The thermal conductivity for the sand-castings (C1 and C2) and the re-melting (C3) experiment is plotted against tensile strength in Figure 5, as well as results from works on the effect of the production parameters on the tensile and thermal properties of different cast iron grades.[14–19] These works analyzed how the thermal conductivity and tensile strength are affected by the inoculation,[14] CE and Mo contents,[15] graphite sphericity,[16] nodularity and microstructure constituents.[17–19] The very small p value indicates the statistical significance of the relationship obtained. The results show a high coefficient of determination R^2, meaning that there is a high degree of dependency between the two variables.

A regression analysis was conducted on the experimental data, and the obtained empirical model is described by Eqn. 3:

$$\lambda = 1881 \cdot \mathrm{UTS}^{-0.7} \qquad \text{Eqn. 3}$$

where λ is the thermal conductivity, and UTS is the ultimate tensile strength

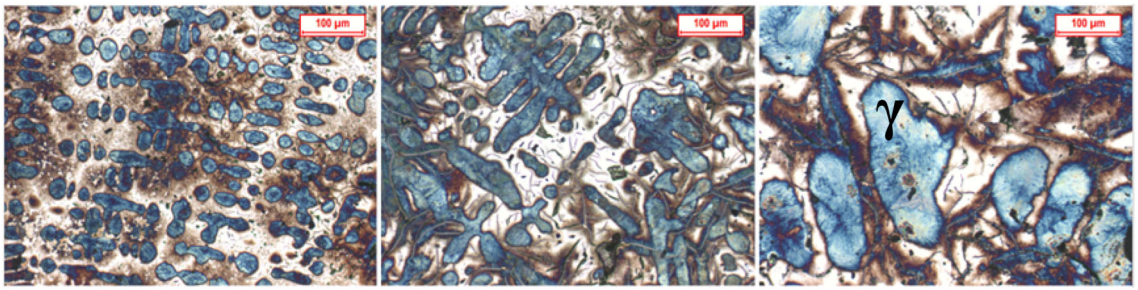

(a) Chill (b) Sand (c) Insulation material

Figure. 2. Micrographs of etched samples from experiment C2 Heat 1.

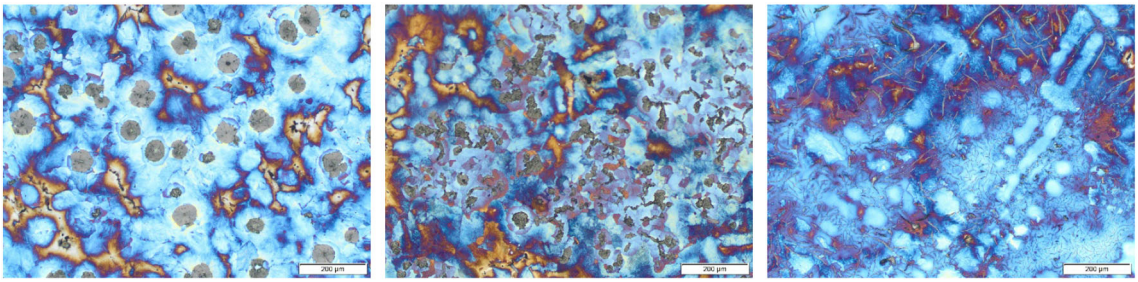

(a) 10 min holding time (b) 60 min holding time (c) 150 min holding time

Figure. 3. Micrographs of etched samples for different holding times at 1450 °C.

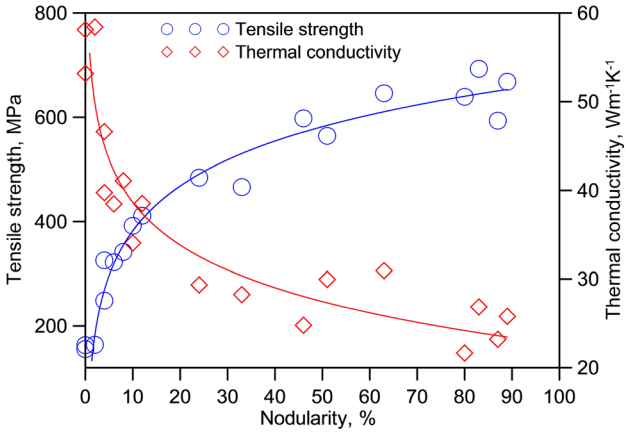

Figure. 4. Tensile strength and thermal conductivity as a function of nodularity for the samples from the re-melting experiments.

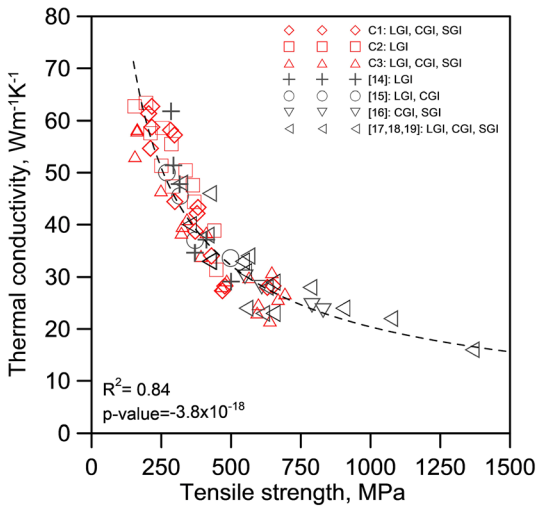

Figure. 5. Thermal conductivity as a function of tensile strength.

The relationship illustrated in Figure 5 is based in a large number of different experimental sources and indicates the existence of a generic relation between thermal conductivity and tensile strength, valid for the range studied in the present paper, regardless of nodularity, matrix constituent, carbon content and solidification rates. It should be stressed that the correlated experimental data have been produced under very different casting, inoculation and heat treatment practices.

The obtained relationship suggests that improved thermal conductivity in cast iron can be achieved at the expense of the tensile strength. This characteristic can be attributed to the opposite effect of the various microstructure features on the investigated properties. Microstructure parameters that improves the tensile strength such as higher nodularity, finer graphite structure, higher primary austenite and pearlite fraction have been also reported to have a harmful effect on the thermal conductivity.

While the data deviation of the fitting line in Figure 5 is partly due to the inevitable uncertainties of the experimental measurements, it also provides an indication of the potential for improving, at the same time, both thermal conductivity and tensile strength. A study[20] has shown that the tensile strength and thermal conductivity of LGI can be improved by 23 and 11%, respectively, by adjusting the amount of the inoculation. Also, the tensile strength can greatly differ for the samples with comparable thermal conductivity in SGI.[7] Future investigations can analyze further the extension of the inoculation effect in relation to other parameters such as nodularity, alloying additions and solidification time.

It is important to consider the validity of the found relationship at higher temperatures where the engine components operate. For this purpose, additional data from[16] are presented in Figure 6. The thermal conductivity and the tensile strength were investigated in[16] for a range of nodularity's and at different temperatures. As can be seen, there is an inverse correlation between tensile strength and thermal conductivity at 200 and 500 °C, verifying that the relationship presented in this work is valid also for higher temperatures, at least for the limited dataset of this study. Further experiments at elevated temperatures are to be performed to calibrate the relationship presented in this paper as a function of the application temperature.

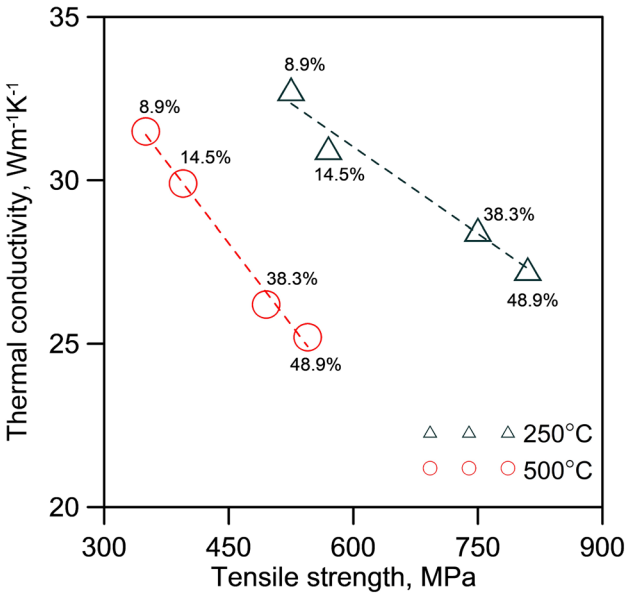

Figure. 6. Thermal conductivity as a function of tensile strength for different nodularity and at different temperatures.[16]

Conclusions

The present results compile the tensile and thermal properties of cast iron produced under a wide variety of influential parameters found in the literature. The result shows the existence of a generic relationship between thermal conductivity and tensile strength valid for the cast iron alloys studied in the present paper, regardless of the graphite shape, matrix constituents, chemical composition, solidification rates, casting methods, inoculation and heat treatment practices. This relationship indicates the challenges for the simultaneous optimization of the thermal conductivity and tensile strength during the development of cast iron alloys for elevated temperature applications.

Acknowledgements

This research was funded by Swedish Knowledge Foundation through the research project Lean Cast, grant number (20180033). Cooperating parties in the project are Jönköping University, Scania CV AB, Sinter Cast AB, SKF Mekan AB, and Volvo Group Trucks Technology AB. The authors gratefully acknowledge all support and participating personnel from the above institutions. Particular acknowledgment is directed toward David Palomo and Patricia Alonso for their contribution to the experimental work reported in the present study.

Funding

Open access funding provided by Jönköping University.

Conflict of interest The authors declare that they have no known competing financial interests or personal relationships that could have appeared to influence the work reported in this paper.

REFERENCES

1. D. Pierce, A. Haynes, J. Hughes, R. Graves, P. Maziasz, G. Muralidharan, A. Shyam, B. Wang, R. England, C. Daniel, High temperature materials for heavy duty diesel engines: Historical and future trends. Prog. Mater Sci. **103**, 109–179 (2019)
2. Y. Park, R. Gundlach, R. Thomas, J. Janowak, Thermal fatigue resistance of gray and compacted graphite irons. AFS Trans. **93**, 415–422 (1985)
3. K. Roehrig, Thermal fatigue of gray and ductile irons. AFS Trans. **86**, 75–88 (1978)
4. S.N. Lekakh, V.A. Athavale, L. Bartlett, M. Li, Effect of micro-structural dispersity of SiMo ductile iron on thermal cycling performance. Inter Metalcast (2022). https://doi.org/10.1007/s40962-022-00915-5
5. S.N. Lekakh, C. Johnson, L. Godlewski, M. Li, Control of high-temperature static and transient thermomechanical behavior of simo ductile iron by Al alloying. Inter. Metalcast. (2022). https://doi.org/10.1007/s40962-022-00768-y
6. J. Helsing, G. Grimvall, Thermal conductivity of cast iron: Models and analysis of experiments. J. Appl. Phys. **70**, 1198–1206 (1991)
7. J. R. Davis, (Ed.). (1996). ASM specialty handbook: cast irons. ASM international
8. D. Holmgren, I.L. Svensson, Thermal conductivity–structure relationships in grey cast iron. Inter Metalcast **18**(6), 321–330 (2005). https://doi.org/10.1179/136404605225023162
9. D. Holmgren, A. Diószegi, I.L. Svensson, Effects of transition from lamellar to compacted graphite on thermal conductivity of cast iron. Inter Metalcast **19**(6), 303–313 (2006). https://doi.org/10.1179/136404607X176203
10. V. Fourlakidis, A. Diószegi, A generic model to predict the ultimate tensile strength in pearlitic lamellar graphite iron. Mater. Sci. Eng. A **618**, 161–167 (2014)
11. J.C. Hernando, J. Elfsberg, E. Ghassemali, A.K. Dahle, A. Diószegi, The role of primary austenite morphology in hypoeutectic compacted graphite iron

alloys. Inter. Metalcast. **14**, 745–754 (2020). https://doi.org/10.1007/s40962-020-00410-9
12. V. Fourlakidis, I. Belov, A. Diószegi, Strength prediction for pearlitic lamellar graphite iron: model validation. Metals **8**, 684 (2018)
13. J.C. Hernando, B. Domeij, D. González, J.M. Amieva, A. Diószegi, New experimental technique for nodularity and mg fading control in compacted graphite iron production on laboratory scale. Metall. and Mater. Trans. A. **48**(11), 5432–5441 (2017)
14. G. Wang, X. Chen, Y. Li, Z. Liu, Effects of inoculation on the pearlitic gray cast iron with high thermal conductivity and tensile strength. Materials **11**(10), 1876 (2018)
15. W.L. Guesser, I. Masiero, E.C.C.S. Melleras, Thermal conductivity of gray iron and compacted graphite iron used for cylinder heads. Revista Matéria **10**(2), 265–272 (2005)
16. Y. Liu, Y. Li, J. Xing, S. Wang, B. Zheng, D. Tao, W. Li, Effect of graphite morphology on the tensile strength and thermal conductivity of cast iron. Mater. Charact. **144**, 155–165 (2018)
17. K. Jalava, K. Soivio, J. Laine, J. Orkas, Elevated temperature thermal conductivities of some as-cast and austempered cast irons. Mater. Sci. Technol. **14**, 327–333 (2018)
18. K. Jalava, K. Soivio, J. Laine, J. Orkas, Effect of silicon and microstructure on spheroidal graphite cast iron thermal conductivity at elevated temperatures. Inter. Metalcast. **12**, 480–486 (2018). https://doi.org/10.1007/s40962-017-0184-1
19. J. Laine, K. Jalava, J. Vaara, K. Soivio, J. Orkas, The mechanical properties of ductile iron at intermediate temperatures: the effect of silicon content and pearlite fraction. Inter. Metalcast. **15**, 538–547 (2021). https://doi.org/10.1007/s40962-020-00473-8
20. A. Diószegi, V. Fourlakidis, J.C. Hernando, D. Holmgren, Effect of inoculation on the material property in cast iron, oral presentation by Diószegi at the 74th World Foundry Congress, Busan, Korea, 2022.